ARTICLE NO. 79-1464R

J80-230

Adaptive Grid Method for Problems in Fluid Mechanics and Heat Transfer

20005

H. A. Dwyer*
University of California, Davis, Calif.
and
R. J. Kee† and B. R. Sanders‡
Sandia Laboratories, Livermore, Calif.

A new method for generating adaptive grids for time-dependent and steady problems in multidimensional fluid mechanics and heat transfer has been developed. The method can be used with many existing grid generation schemes or can be used as an independent grid generation technique. The present adaptive method is based upon the placement of grid points in proportion to the gradients that appear in the dependent variable. The multidimensional results presented in the paper are for the unsteady heat conduction equation and have included steep gradients due to geometry and unsteady boundary conditions. The method has performed in an impressive fashion, although there is a need to control grid skewness better. A study of one-dimensional problems associated with combustion and cell Reynolds number has demonstrated the technique's accuracy and versitility. The paper also discusses the relationship of the method to other grid generation techniques, as well as extensions of the new method.

Introduction

IN this paper an adaptive grid method has been proposed and deveoped for multidimensional problems in fluid mechanics and heat transfer. An interesting feature of the scheme is that it adjusts the finite-difference grid to the solution of the transport equation being solved. This feature is particularly important in time-dependent and nonlinear problems where the dependent variable gradients are not known a priori. The method also has the attractive feature that it can be used with most present grid generation methods as an added feature. Also, since the method uses information on the dependent variable in the problem, attractive features based on physics are rendered in some situations.

One of the more difficult problems facing the numerical modeler in fluid mechanics and heat transfer is the lack of a priori information concerning the gradients in the dependent variables to be calculated. Without this information the grid used in many numerical solutions is usually wasteful, and does not resolve satisfactorily those important regions where gradients exist. Unfortunately, this is damaging to the numerical simulation itself, since important physical phenomenon do occur in high gradient regions. Over the past few years there has been significant progress made in acquiring the tools necessary to tackle the grid generation problem. Two of the most important tools are: 1) a statement of the basic transport equations in a nonorthogonal strong conservation form,[1,2] and 2) the development of a variety of grid generation schemes for complicated geometries.[3-5] The paper by Steger[5] is representative of these methods as they are currently being employed, and that paper also addresses in a nonadaptive way the resolution of high gradient regions.

Presented as Paper 79-1464 at the AIAA 4th Computational Fluid Dynamics Conference, Williamsburg, Va., July 23-24, 1979; submitted Sept. 21, 1979; revision received Jan. 21, 1980.

Index category: Computational Methods.

*Professor. Member AIAA.
†Supervisor, Applied Mathematics.
§Supervisor, Gas Dynamics Division.

The problem of the resolution of high gradient regions in fluid mechanics and heat transfer is important not only for truncation error considerations, but also from the physical point of view. Due to nonlinear phenomena associated with physical parameters, such as Reynolds number (boundary layers and turbulence), Mach number (compressibility and shock formation), Damkohler number (chemical reactions), and others, there is a tendency for the most important physical processes to occur in very thin regions. These regions may or may not be associated with boundaries and can also be moving about in time. In order to have an accurate physical simulation of these "boundary-layer" regions, the finite-difference grid system must resolve them; and since their locations are not known a priori, an adaptive type of grid should be employed. In the remainder of the paper a method of resolving high gradient regions for multidimensional problems will be developed and examples from various physical phenomena given.

Criterion for Grid Placement

The basic criterion for grid placement used in this paper will now be developed. A good practice is that all calculations be carried out in a normalized computational space which will be fixed in time, as shown in Fig. 1. In the physical space grid points will be placed and moved in time to achieve the resolution of high gradient regions. In the most general case, lines of constant ξ and η in the computational space will correspond to nonorthogonal arcs in the physical space. Along a given arc in the physical space the grid points will be distributed in proportion to the gradient of the dependent variable. If the distance along a given arc in physical space is denoted by S, a mathematical statement of the relationship between the computational and physical space is

$$d\xi \propto \left| \frac{\partial T}{\partial S} \right| dS \tag{1}$$

where S is the distance measured on the η = constant arc, and T the dependent variable of the transport equation being solved. In order to normalize, allow for "optimization," and

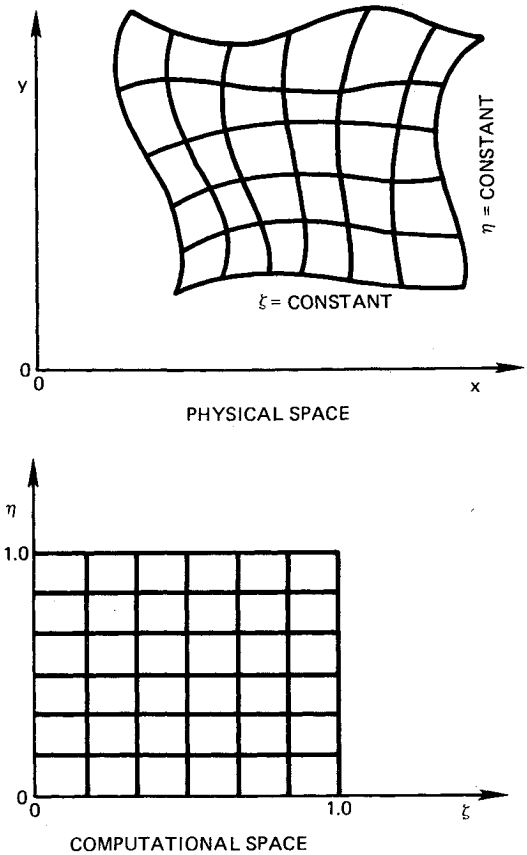

Fig. 1 Schematic of physical and computational spaces.

remove singularities, Eq. (1) is cast into the following form

$$\xi(x,y,t)=\left[\int_0^S\left(1+b\left|\frac{\partial T}{\partial S}\right|\right)\mathrm{d}S\right]\Big/\left[\int_0^{S_{\max}}\left(1+b\left|\frac{\partial T}{\partial S}\right|\right)\mathrm{d}S\right] \tag{2}$$

where b is an adjustable constant used for "optimization" of the grid distribution. (Note: A similar relationship can easily be written for the other nonorthogonal arc.)

Equation (2) has some interesting features which will now be discussed. For the case $b=0$ a uniform distribution of points on the nonorthogonal arc is obtained, while for b becoming large Eq. (2) takes on the following form

$$\xi(x,y,t)=\int_0^S|\mathrm{d}T|\Big/\int_0^{S_{\max}}|\mathrm{d}T| \tag{3}$$

Since grid points are placed at uniform values of ξ, the $S(x,y)$ locations will correspond to constant values of the difference in the dependent variable T. For many heat-transfer and combustion applications this limit can be an attractive feature and it will be discussed in other parts of the paper. Another characteristic of Eq. (2) is that it can underestimate regions where $\partial T/\partial S$ is zero but a large second derivative exists. In order to avoid problems of this type, Eq. (2) can be extended to the following form

$$\xi(x,y,t)=\frac{\int_0^{S_{\max}}\left(1+b\left|\frac{\partial T}{\partial S}\right|+C\left|\frac{\partial^2 T}{\partial S^2}\right|\right)\mathrm{d}S}{\int_0^{S_{\max}}\left(1+b\left|\frac{\partial T}{\partial S}\right|+C\left|\frac{\partial^2 T}{\partial S^2}\right|\right)\mathrm{d}S} \tag{4}$$

where C is a weighting constant (or possible function) that controls the relative importance of second derivative influence on grid distribution. The solution to the above equations is straightforward; however, it is best to discuss this in conjunction with the physical examples to be presented in later sections. Therefore, further discussion of Eq. (2) will be delayed until a more concrete example is developed.

Application to Unsteady Heat Transfer

The adaptive grid procedure just mentioned will now be applied to an unsteady heat-transfer problem. The basic equation for the temperature field can be written as

$$\frac{\partial T}{\partial t}=\alpha\left(\frac{\partial^2 T}{\partial x^2}+\frac{\partial^2 T}{\partial y^2}\right) \tag{5}$$

Under a nonorthogonal transformation to ξ, η, and τ this equation takes on the following strong conservative form[1,2]:

Transformed equation

$$\begin{aligned}\frac{\partial}{\partial\tau}\left(\frac{T}{J}\right)&=-\frac{\partial}{\partial\xi}\left(\frac{\xi_t T}{J}\right)-\frac{\partial}{\partial\eta}\left(\frac{\eta_t T}{J}\right)\\&+\alpha\left[\frac{\partial}{\partial\xi}\left(\frac{\partial T}{\partial\xi}\frac{[\xi_x^2+\xi_y^2]}{J}+\frac{\partial T}{\partial\eta}\frac{[\xi_x\eta_x+\xi_y\eta_y]}{J}\right)\right.\\&\left.+\frac{\partial}{\partial\eta}\left(\frac{\partial T}{\partial\eta}\frac{[\eta_x^2+\eta_y^2]}{J}+\frac{\partial T}{\partial\xi}\frac{[\xi_x\eta_x+\xi_y\eta_y]}{J}\right)\right]\end{aligned} \tag{6}$$

where

$$J=\xi_x\eta_y-\xi_y\quad \eta_x=\frac{1}{(x_\xi y_\eta-x_\eta y_\xi)}$$

$$\xi_x=Jy_\eta\quad \eta_x=-Jy_\xi\quad \xi_t=-x_\tau\xi_x-y_\tau\xi_y$$

$$\xi_y=-Jx_\eta\quad \eta_y=Jx_\xi\quad \eta_t=-x_\tau\eta_x-y_\tau\eta_y$$

With the equation cast in terms of the transformed variables ξ and η finite-difference approximations can be made quite easily since the step size is uniform in the transformed plane. However, all of the difficulty of the geometry and time-dependent grid adaption has now been placed into the metric terms, such as ξ_t, η_t, η_x, ξ_y, etc. At the present time most methods of grid generation (including the present) do not have a good measure of what is a suitable variation of these functions for an accurate solution. For example, as the grid expands from a high gradient region "what constraints should be placed on the expansion," or "when are there significant advantages to orthogonalizing the grid skewness or lack of independence"? The above points and many others will have to be answered in the coming years and will be crucial to the formation of design tools for use in modeling. Therefore, the present result will be somewhat experimental in its use of adpative grids, since these questions have not yet been answered; however, the present adaptive technique does represent an increase in our current abilities.

Some solutions to Eq. (6) will now be presented for some complex geometries. The initial conditions for the problem will be $T=0$ everywhere at $t=0$ and the boundary conditions will consist of one wall being impulsively raised to $T=1$. Because of the impulsive heating and the complex geometry, large gradients appear at various locations and times in the problem. To solve Eq. (6) an ADI scheme with second-order central differences has been employed. To calculate accurately the time-dependent metric terms with second-order accuracy, a predictor step was taken first to determine the change in the transformation. With the transformation determined by this predictor, a Crank-Nicolson type of time differencing was employed to calculate ξ_t and η_t.

A solution of Eq. (6) at an early time to the first problem is shown in Fig. 2, and is mainly presented for illustration. The coordinate system is given in the left-hand figure and the isotherms in the right. Boundaries for the upper and lower walls were chosen as sinusoidal distributions while the side walls are straight. The initial distribution of coordinates (not shown) for $t=0$ consisted of uniformly spaced grids between the upper and lower boundaries. In these first examples adaption was carried out only along one of the coordinates and this can be justified in many problems; however, there is no inherent restriction in the method to one coordinate. (This point will be discussed more fully as the paper develops.) The grid points were moved along the $\xi=$ constant line (or vertical lines) as the gradients developed in accordance with Eq. (2).

As can be seen from Fig. 2, both the isotherms and grid system are bunched near the lower wall at this early time in the solution. For the results presented, a value of $b=0.333$ was chosen from numerical experimentation. The procedure for solving Eq. (2) was by quadrature along $\xi=$constant. Uniformly spaced values of η, between 0 and 1, are placed on the left-hand side of Eq. (2) and a quadrature is performed on the right to locate points in physical space. For example, the location in physical space of the $\eta=0.5$ would be found from the following sum

$$0.5=\frac{\sum_{i=1}^{S(\eta=0.5)}\left(\Delta S+b\left|\frac{\Delta T}{\Delta S}\right|\right)\Delta S}{\sum_{i=1}^{S_{\max}}\left(\Delta S+b\left|\frac{\Delta T}{\Delta S}\right|\right)\Delta S} \tag{7}$$

where S is the arc length. In most applications the S location of $\eta=0.5$ lies between old points and must be found by interpolation. However, high-order formal accuracy is not needed in the solution of Eq. (7) since the grids need be placed only in the vicinity of large dependent variable gradients. Therefore, a first order solution is usually more than adequate, and the amount of time involved in determining new grid locations is quite small.

The solution presented in Fig. 2 represents the results after ten time steps and three grid adaptions. The grid was adaptive at the $t=0^+$ and every four time steps thereafter. It was found that more accurate solutions were obtained without adapting every step, and this feature was the result of oscillations that can occur between grid adaption and the solution. By allowing for a more definite change in the depended variable, these grid adaption-solution oscillations did not occur. Also, it should be mentioned that steady-state solutions would require even fewer time-dependent adaptions, and the amount of adaption will depend on Δt and the solution itself.

It can be seen from Fig. 2 that the original uniformly spaced grid has been expanded and compressed in order to place grid points near the high gradient wall. The grid spacing near the wall was less than 1/10 the original spacing, and could be made smaller by increasing the value of b or decreasing Δt. There is an optimum value of b to obtain the most accurate solution, and the accuracy degraded as b was changed from this value. A detailed discussion of accuracy will be given in a later section after some examples are presented.

A later time in the solution is shown in Fig. 3 where the isotherms have moved further from the heated wall, and the grid also has moved away from the wall. An interesting feature of this result is the grid bunching near the end points of the impulsively heated wall. In this solution, adaption was not carried out on the walls itself, and the wall points were given the same relative grid distribution as their nearest neighbor. The difficulty with adapting along the wall is that grid points move closer to the end-point singularity on every time step in an attempt to resolve the singularity. The integral in Eq. (2) remains well-behaved, but ΔS becomes smaller than the machine capacity and the calculation terminates.

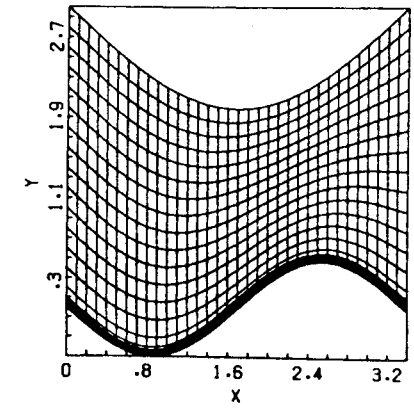

Fig. 2 Eddy time coordinates and isotherms.

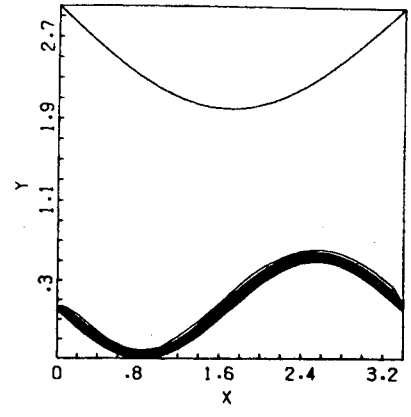

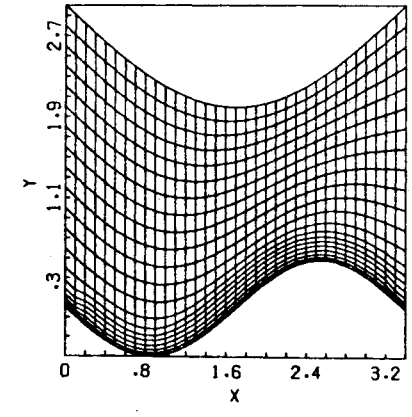

Fig. 3 Intermediate time coordinates and isotherms.

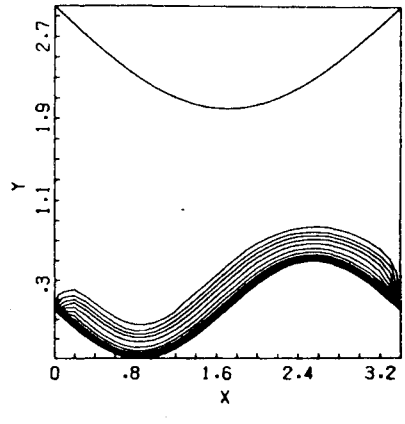

A calculation with a more distorted wall and grid adaption along the side walls is shown in Figs. 4 and 5. The long-time solution in Fig. 5 (essentially steady state) has extreme adaption near the two singularities. The amazing part of the calculation is that not all side wall nodes are bunched near the

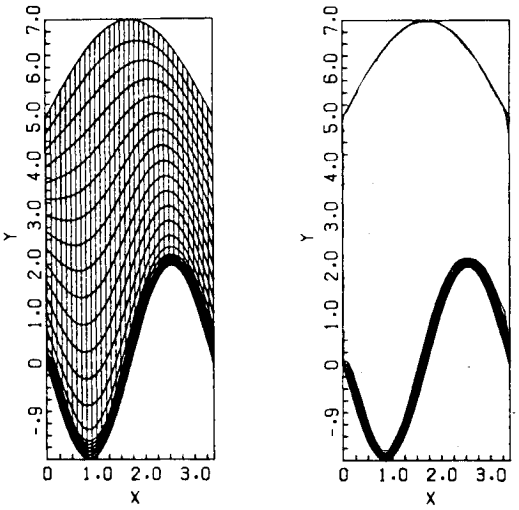

Fig. 4 Early time coordinates and isotherms.

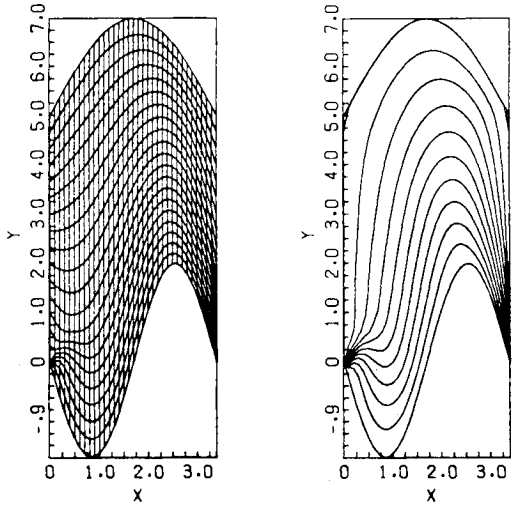

Fig. 5 Steady-state coordinates and isotherms.

singularity, and that the side wall step size (ΔS) at the first node away from the singularity is less than 1.10^{-20}. It was difficult to test the accuracy of the result formally (due to lack of something to compare the numerical solution against), but the solution seems to agree with physical intuition as can be seen from the isotherm distribution. However, Figs. 4 and 5 are good examples of grid adaption to complex geometries and boundary conditions with a simple method that does not substantially increase computational time.

At this point it is appropriate to compare the present method with other techniques. One of the more popular grid generation methods is the elliptic solver developed by Thompson.[3] In this method the termination points of the coordinates on the boundaries would be chosen a priori, and an elliptic equation of the Poisson type solved to determine the coordinate locations throughout the solution region. These coordinates will not in general be orthogonal and limited control of coordinate location in the interior is obtained. However, they do have the feature that they fit the boundaries and lines of constant ξ or η do not cross. These solvers could be used for the problems presented in Fig. 2-5 to obtain an initial distribution and adaption could then be carried out along one of the arcs. In many problems this procedure will be a useful one; however, in many other problems an initial distribution of coordinates can be chosen by inspection. For example, approximate streamlines or heat-flow lines could be chosen for initial conditions and fitted

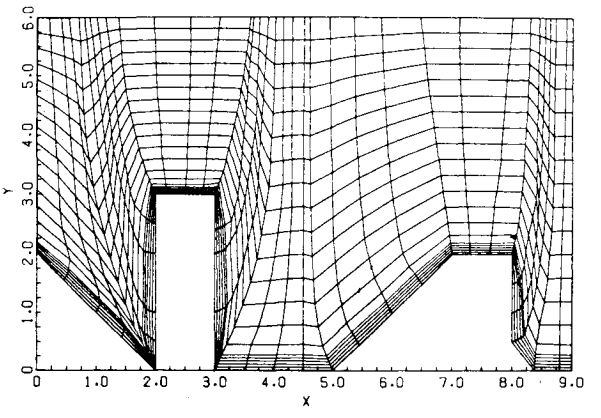

Fig. 6 Early time coordinate system.

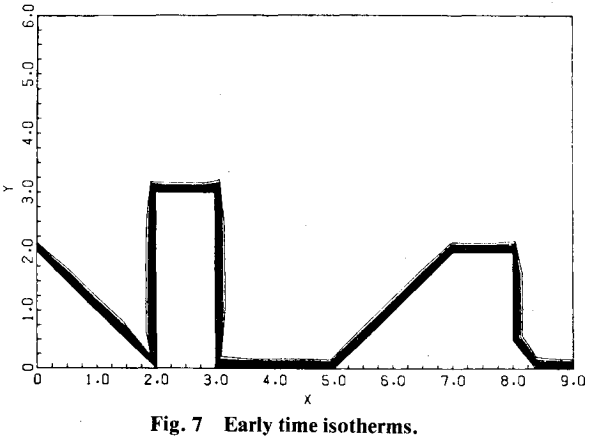

Fig. 7 Early time isotherms.

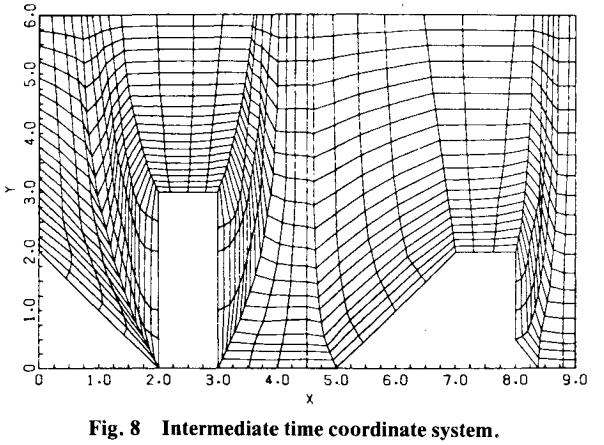

Fig. 8 Intermediate time coordinate system.

with splines or another method and adaption carried out as the solution develops.

An example of the latter type of procedure is shown in Figs. 6-9 for a rather complex shape. For this problem the initial and boundary conditions are the same as the previous examples; however, the lower boundary has a rather jagged shape. The initial coordinates were found by drawing continuous straight lines from the lower to upper boundary, and the grid points spaced uniformly along these arcs. The arcs were given the property of leaving the lower boundary with an approximate right angle (it should be remembered that the heat flux is perpendicular to a constant temperature wall) and did not cross themselves. The initial arcs were chosen as straight lines only for simplicity and to demonstrate the robustness of the technique. (A better method would be to fit splines or other polynomials that would have continuous derivatives.)

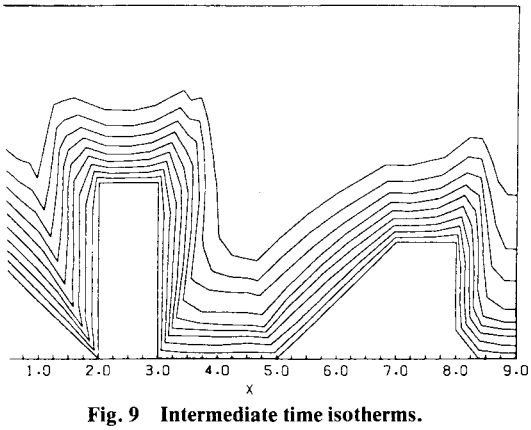

Fig. 9 Intermediate time isotherms.

The results in Figs. 6 and 7 are for an early time in the heat-transfer process, and it can be seen that the grid has adapted nicely to the high gradient region near the wall. An interesting feature of the grid in Fig. 6 is the high skewness and rapid turning due to limited grid location and very complex geometry. It is a logical question to ask whether the metric terms would undermine the accuracy of the solution. The major reason for the solution being accurate is that the adaptive procedure has chosen something close to isotherms for lines of $\eta =$ constant. Therefore, derivatives such as $\partial T/\partial \xi$ are small and the cross-derivatives are also small. The problems of skewness and lack of dependence are not as severe if the coordinate lines coincide with constant values of the dependent variables. This observation leads one to reassess the concept of natural coordinates as it has been used for grid generation.

Previous studies have defined natural coordinates as body fitted, but this definition seems to be somewhat incomplete. For a coordinate system to be natural it should reflect boundary conditions, boundary geometry, and internal gradients. Such phenomena as variable wall conditions, flame propagation, and internal shear layers should exert a major influence on the coordinate location. The grid transformations we have developed is a step in achieving this goal as can be seen from the adaption to complex geometry and boundary conditions given in Figs. 2-9.

It is now time to address some of the difficulties with this new technique. A major problem seems to be the lack of control of grid skewness throughout the solution region. For example, the solutions presented in Figs. 8 and 9 were the last ones in time that did not develop oscillations in the grid and solution due to skewness. The oscillations could be controlled by taking smaller time steps, but the computational time then increases considerably. The solution to this problem seems to be available but has not yet been implemented. This attractive remedy has been worked out in a paper by Potter and Tuttle,[4] where they devised a procedure for constructing an orthogonal grid from one set of coordinate lines. The method has been demonstrated to handle complex geometries and is independent of coordinate spacing, as well as being computationally inexpensive. It is envisioned that the present adaptive procedure will determine one set of coordinates based upon the solution itself, while the Potter and Tuttle procedure will find an orthogonal set to match the adaptive coordinates. For many problems, this coordinate system will be natural, since gradient regions and boundaries will be resolved. If lines of constant T are found by the adaptive procedure, then the other set will correspond to the direction of the heat flux vector, while for incompressible viscous flow a similar procedure could be used to locate streamlines.

Another problem that remains to be more fully resolved is the application of derivative boundary conditions. The use of first-order approximations caused excessive movement of boundary grid locations near high gradient regions. At the present time further research is being carried out in this as well as grid orthogonalization. The accuracy of this time-dependent adaptive procedure is another question, and the following section will be devoted to this important topic.

Accuracy with Grid Adaption

There are two important places where an adaptive grid procedure can influence the accuracy of a finite-difference calculation. These places are the location of coordinates based on gradients, and the generation of rapid variation of metrics in two and three dimensions. The two problem areas are not independent; however, it is convenient to separate the problems of complex geometry from grid location. There will now be presented two time-dependent one-dimensional examples which test severely the problem of grid location. The second problem of grid geometry is too ambitious to be tackled in a comprehensive way at this time.

The first problem to be calculated is concerned with flame propagation and is highly nonlinear. The problem to be solved is concerned with flame propagation in a solid without gas generation and has been studied extensively by Otey and Dwyer[6] without grid adaption. The basic equations in the transformed plane are

$$\frac{\partial \rho_A}{\partial \tau} = -\frac{\partial \rho_A}{\partial \xi}\xi_t + \frac{\partial}{\partial \xi}\left(\xi_x \frac{\partial \rho_A}{\partial}\right)\xi_x - A_1 e^{-\theta_1/T}$$

$$\frac{\partial T}{\partial \tau} = -\frac{\partial T}{\partial \xi}\xi_t + \frac{\partial}{\partial \xi}\left(\xi_x \frac{\partial T}{\partial \xi}\right)\xi_x + A_1 e^{-\theta_1/T} \qquad (8)$$

where x and t are physical coordinates, ξ and τ transformed, ρ_A and T the species density and temperature, and A_1 and θ_1 constants characteristic of the combustion process.

Some of the most sensitive processes in the solution of Eq. (8) are the flame speed and the ignition process. If a uniform grid is employed to solve for these fast thin flames, a very large number of grid points are needed to have an accurate calculation. For example, Otey and Dwyer[6] needed 600 grid points to calculate accurately the solution for $A_1 = 4.10^7$ and $\theta_1 = 4$ (characteristic of some hydrocarbon combustion). To carry out the same calculation with comparable accuracy and with the adaptive grid ($b = 0.333$) required only 50 grid points. This was a savings of over one order of magnitude in the number of grid points and also one order of magnitude in computer time (the dimensionless flame speed was $V_1 = 476$).

Some details of the calculation are shown in Figs. 10-15. (Results have been shown for 50 grid points with and without adaption.) Figure 10 shows the temperature in the physical plane near the right-hand boundary immediately after the wall has started the ignition process. The solid line represents the adaptive solution, while the circles correspond to the uniform grid solution without adaption. Ignition has not occurred in the uniform grid solution because the first grid point is too far from the wall.

In Fig. 11 the distribution of temperature in the transformed coordinates at this instant is shown, and it can be easily seen by comparing Figs. 10 and 11 that the adaptive procedure makes efficient use of grid locations. An interesting feature of the calculation is shown in Fig. 12 where the step size (Δx) in the physical space is plotted against the transformed coordinate. It should first be noticed that the physical step size varies over two orders of magnitude for this converged and accurate calculation. One feature that is not so attractive is the rapid rise of Δx near the location of the maximum temperature. At the maximum $\partial T/\partial x = 0$ and the step size tends to increase. The remedy to this problem has already been given in Eq. (4) where a second-derivative influence has been added ($\partial^2 T/\partial x^2$ is quite large at the temperature maximum).

A later time in the process is shown in Figs. 13-15. Figure 13 shows the fully developed flame temperature profile for

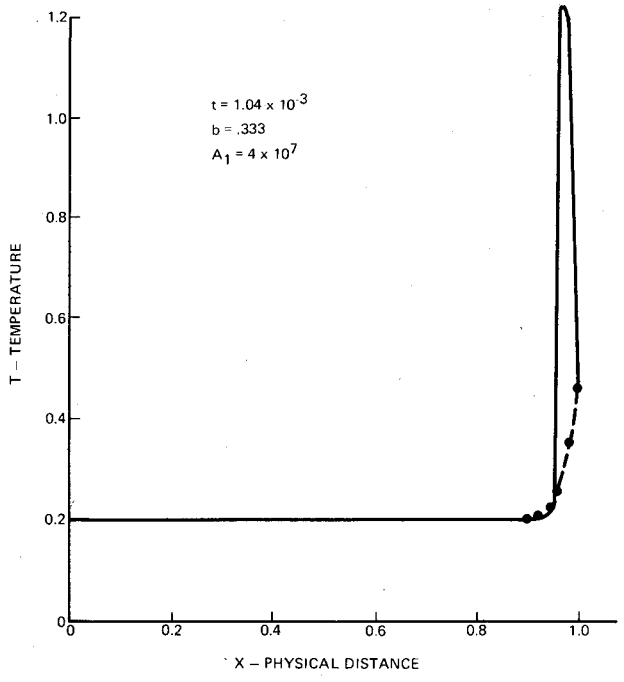

Fig. 10 Temperature profile at ignition in physical plane.

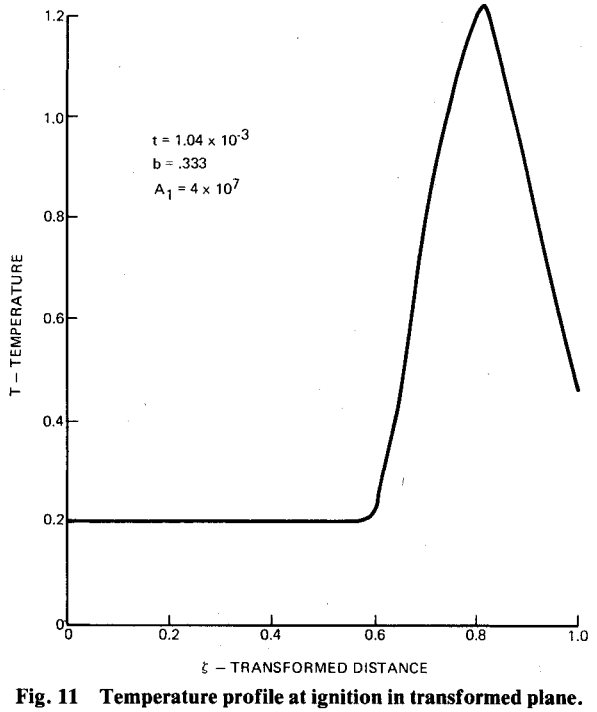

Fig. 11 Temperature profile at ignition in transformed plane.

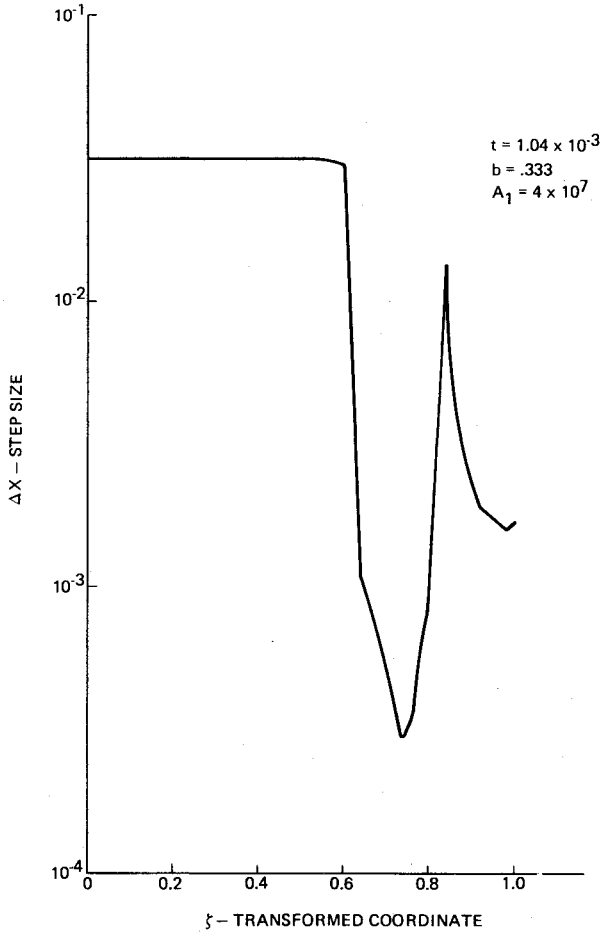

Fig. 12 Physical plane step-size variation at ignition.

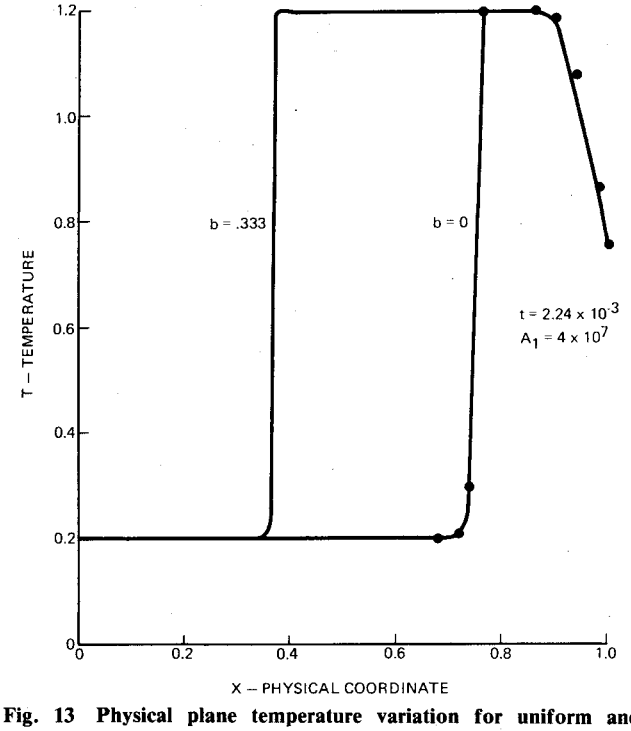

Fig. 13 Physical plane temperature variation for uniform and adaptive grids.

adaptive and uniform grid solutions. The uniform grid solution is lagging badly behind even though the profile looks reasonable (only one grid point was in the gradient region). It should also be noted that a wall quench layer exists at $x = 1.0$, and this has introduced another scale in the problem. The distribution of temperature in the transformed plane (Fig. 14) exhibits how nicely the adaptive procedure has treated the two separate scales associated with the flame and the quenched layer. The distribution of step size in the transformed plane is shown in Fig. 15, and it is seen again how the size varies with the gradients in the problem.

The above results show quite clearly that the adaptive procedure can calculate ξ_t and ξ_x accurately and also place the grid points where needed. However, it should be mentioned again that the problem of skewness in multiple-space dimensions has not been completely studied. But it is also clear that the present adaptive technique shows definite promise.

The second problem is concerned with "cell Reynold's number" restrictions which appear in most viscous flow and transport processes. The example chosen is from Roache[7] and

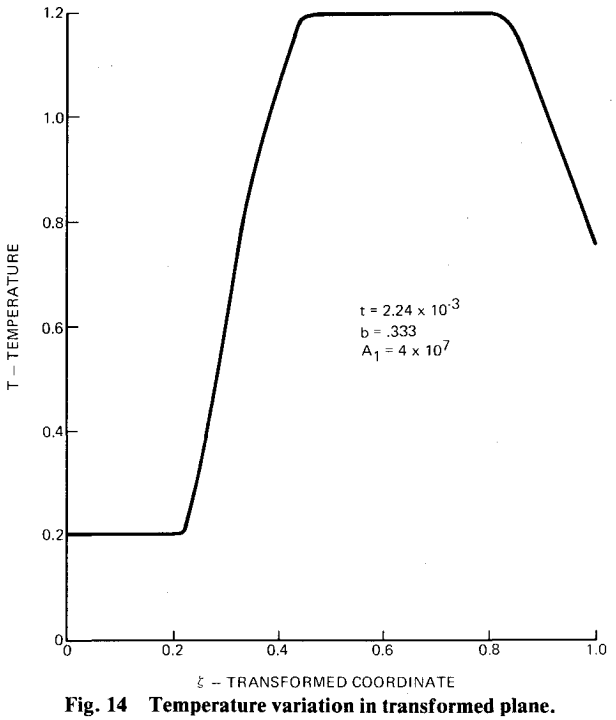

Fig. 14 Temperature variation in transformed plane.

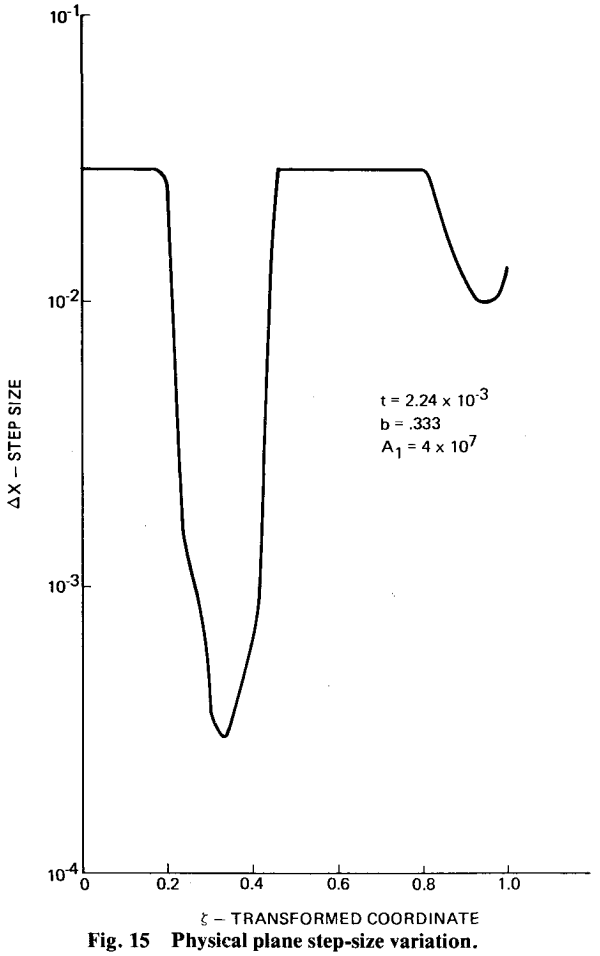

Fig. 15 Physical plane step-size variation.

the basic equation of the model problem is

$$\frac{\partial v}{\partial t} = -\frac{\partial v}{\partial \xi}\xi_t - U\frac{\partial v}{\partial \xi}\xi_x + \frac{\partial}{\partial \xi}\left(\xi_x \frac{\partial v}{\partial \xi}\right)\xi_x \qquad (9)$$

For large values of $Re = U/\alpha$ a finite-difference solution will exhibit severe oscillations due to lack of resolution of high

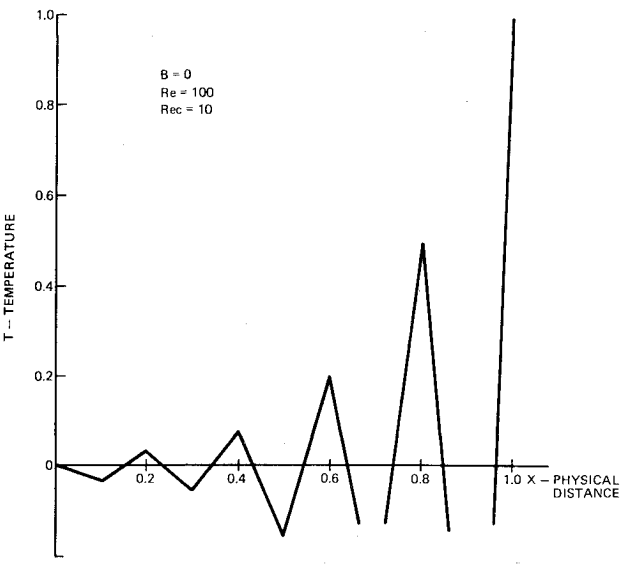

Fig. 16 Cell Reynold's number problem with oscillations.

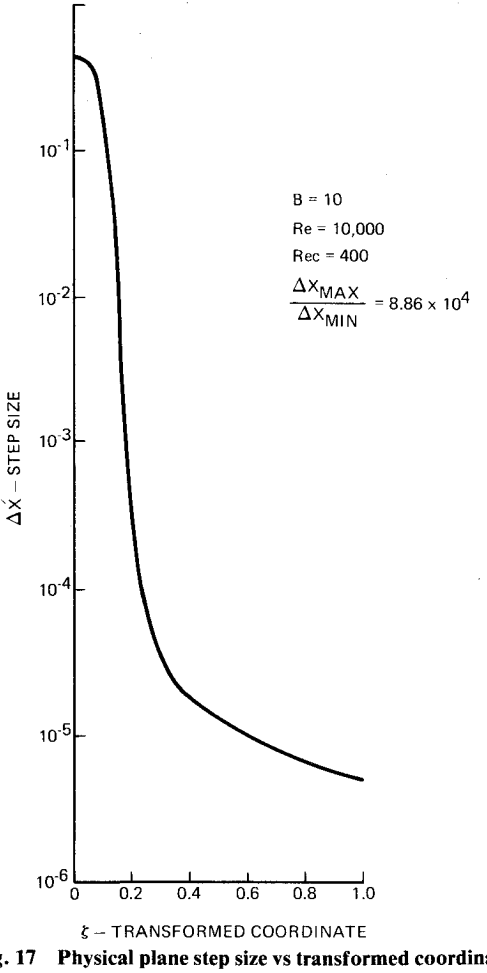

Fig. 17 Physical plane step size vs transformed coordinate.

gradient regions. The severity of the oscillations or the degradation of the solution depends upon the finite-difference method, but the problem exists for most methods. An example case with central difference approximations to all terms in Eq. (9) is shown in Fig. 16 for a uniform grid of ten points and $Re = 100$. (The cell Reynold's number is therefore $Re_c = 10$.) The actual steady solution for the boundary condition $v = 0$ at $x = 0$ and $v = 1$ at $x = 1$ consists of an extremely steep line near the boundary $x = 1$. As can be seen, there is very little correspondence with the numerical solution for this case.

Table 1 Cell Reynolds number problem adaptive grid

B = 10		Re = 10,000	Re_c = 400	$\Delta x_{max}/\Delta x_{min} = 8.862 \cdot 10^4$
ξ	x	Δx	v	$(v_N - v_A)/v_B \times 100$
0	0			0
1/25	0.4431	0.4431	0.00497	0.497
2/25	0.8242	0.3811	-0.013317	-1.3317
3/25	0.9715	0.1473	0.00979	0.979
4/25	0.999167	0.027667	-0.011592	-1.159
5/25	0.999650	0.000483	0.02568	-0.6913
6/25	0.999758	0.000108	0.08740	-0.162
7/25	0.999801	0.000043	0.13478	-0.1244
8/25	0.999830	0.000029	0.18213	-0.1039
9/25	0.999853	0.000023	0.23010	-0.0896
10/25	0.999872	0.000019	0.27819	-0.0790
11/25	0.999888	0.000016	0.32646	-0.0705
12/25	0.999902	0.000014	0.37466	-0.0627
13/25	0.999914	0.000012	0.42291	-0.0568
14/25	0.999925	0.000011	0.47110	-0.0530
15/25	0.999935	0.000010	0.51931	-0.0455
16/25	0.999943	0.000008	0.56748	-0.0393
17/25	0.999952	0.000009	0.61568	-0.0352
18/25	0.999959	0.000007	0.66387	-0.0296
19/25	0.999966	0.000007	0.71211	-0.0260
20/25	0.999973	0.000007	0.76037	-0.0212
21/25	0.999979	0.000006	0.80871	-0.0157
22/25	0.999985	0.000006	0.85703	-0.0092
23/25	0.999990	0.000005	0.90522	-0.0078
24/25	0.999995	0.000005	0.95295	-0.019
25/25	1.0	0.000005	1.0	0

An adaptive solution with central differences for this type of problem was carried out, and the results shown in Table 1 and Fig. 17. A value of $Re = 10{,}000$ was chosen and a total of 25 grid points were used (for a uniform grid $Re_c = 400$). Table 1 shows the variation of x, Δx, v, and error present in v as a function of ξ. The first grid location has been located at a normalized distance of 0.000005 away from the wall, and the variation in step size is enormous, from Fig. 17, where Δx vs ξ is plotted, it is seen that the variation of Δx is over five orders of magnitude. In order to achieve this variation, the value of b had to be raised to 10 so that the sensitivity to gradient was increased; however, the accuracy has not been degraded substantially as seen from Table 1. The maximum error in the value of v is less than 1.5% of the implied boundary condition, and this is doing very well considering the severity of the problem being solved.

Although the cell Reynold's number problem is not a practical consideration in some flow calculations, it is fundamental to two important phenomena—those being "separation" and "flame propagation" with expansion. Therefore, it is very encouraging to see these results.

Discussion of Adaptive Grid Criterion

It has been shown in the previous sections that the criterion we have chosen for adaption has led to substantial reduction in the number of grid points needed for an accurate solution and to the selection of natural coordinates for multidimensional grids. A major objection from the mathematical point of view is that the method is heuristic and does not have a formal way of controlling error. It is possible that a formal minimization procedure can be worked into Eq. (4). The authors are working on this, but it is their belief that heuristic methods will play a large role in computational fluid dynamics. The reason for this belief is centered on the very rich and complex physics that fluid flows exhibit. For example, inside of a flame the temperature gradient is uniform and it is quite easy to make a finite-difference approximation for the distribution. There is no large truncation error associated with this region, but there is a definite need for grid points to be clustered in the flame to resolve the chemical reactions. Therefore, the very promising scheme of Pierson and Kutler,[8] which is based on minimizing truncation error proportional to the third derivative, will be of limited value for this problem. The list of problems in combustion, viscous flow, and turbulence is long where heuristic analysis is needed, and the placement of points based on the value of the dependent variable and its derivative will be a good way to choose grid locations. However, it is always good practice to try continually to bring the physics and formal accuracy control together, and methods such as Pierson's and Kutler's will be valuable in the process.

Conclusions

The adaptive grid procedure developed in the present paper has shown itself to reduce substantially the number of grid points necessary to achieve accurate solutions in fluid mechanics and heat transfer. This reduction has occurred for a wide variety of problems which had complicated geometry, time-dependent gradients, and large steady-state gradients. For the "cell Reynold's number problem" the ratio of the maximum-to-minimum step size in the physical plane was 10^5 with 1% accuracy. When applied to a very nonlinear problem of flame propagation, the method reduced the number of grid points and computation time by an order of magnitude with comparable accuracy. Finally, the method impressively treated complex geometries and steep time-dependent gradients for unsteady heat-transfer problems. An added feature of the technique was the "natural coordinate system" that was chosen by adaption. This coordinate system had the property that the cross-derivative terms were small and rapid metric variation was suppressed in the transport equation. The major difficulty with the method was the lack of control of grid skewness; however, an efficient and effective remedy appears to be available in the orthogonalization method of Potter and Tuttle.[4] The next phase of the research will entail the formation of natural orthogonal grids that adapt to the gradients in the solution.

References

[1] Peyret, R. and Viviand, H., "Computation of Viscous Compressible Flows Based on the Navier-Stokes Equations," AGARD-AG-212, 1975.

[2] Vinokur, M., "Conservation Equations of Gasdynamics in Curvilinear Coordinate Systems," *Journal of Computational Physics*, Vol. 14, No. 2, 1974, pp. 105-125.

[3] Thompson, J. F., Thames, F. C., and Mastin, C. M., "Automatic Numerical Generation of Body-Fitted Curvilinear Coordinate Systems for Fields Containing any Number of Arbitrary Two-Dimensional Bodies," *Journal of Computational Physics*, Vol. 15, July 1974, pp. 299-319.

[4] Potter, D. E. and Tuttle, G. H., "The Construction of Discrete Orthogonal Coordinates," *Journal of Computational Physics*, Vol. 13, 1973, pp. 483-501.

[5] Steger, J. L., "Implicit Finite-Difference Simulation of Flow About Arbitrary Two-Dimensional Geometries," *AIAA Journal*, Vol. 16, July 1978, pp. 679-686.

[6] Otey, G. and Dwyer, H. A., "A Numerical Study of the Interaction of Fast Chemistry and Diffusion," *AIAA Journal*, Vol. 17, June 1979, pp. 606-613.

[7] Roache, P., *Computational Fluid Dynamics*, Hermosa Publishers, Albuquerque, N. Mex., 1971.

[8] Pierson, B. L. and Kutler, P., "Optimal Nodal Point Distribution for Improved Accuracy in Computational Fluid Dynamics," AIAA Paper 79-0272, Jan. 1979.